Structural and Dynamic Properties of the F_v Fragment and the Single-Chain F_v Fragment of an Antibody in Solution Investigated by Heteronuclear Three-Dimensional NMR Spectroscopy†

Christian Freund,‡ Alfred Ross,‡ Andreas Plückthun,§ and Tad A. Holak*,‡

Max Planck Institute for Biochemistry, D-82152 Martinsried, FRG, and Department of Biochemistry, University of Zürich, Winterthurerstrasse 190, CH 8057 Zürich, Switzerland

Received December 6, 1993; Revised Manuscript Received January 10, 1994®

ABSTRACT: F_v fragments, heterodimers of the variable light (V_L) and variable heavy chain (V_H) domains, are the smallest functional antibody units with molecular masses of ~26 kDa. The structural and dynamic properties of the F_v fragment and the corresponding single-chain F_v fragment (scF_v: V_H–linker–V_L, 252 amino acids) of the phosphorylcholine-binding antibody McPC603 in the presence of hapten have been studied in solution by heteronuclear multidimensional NMR spectroscopy. Both ^{15}N TOCSY-HMQC and triple-resonance experiments (HNCA and HN(CA)H, with ^{15}N–^{13}C-labeled protein) gave poor spectra, due to short T_2 relaxation times for most of the backbone ^1H, ^{15}N, and $^{13}C^{\alpha}$ atoms. The assignment procedure therefore relied upon the combination of amino acid and domain (V_L) specifically labeled spectra and the 3D NOESY-HMQC spectrum of the uniformly ^{15}N labeled F_v and scF_v fragments. Approximately 80% of the ^{15}N and ^1H backbone and 60% of the ^1H side-chain resonances have been assigned. Short- and long-range NOEs were used to determine the extent of β-sheet structure and were compared to the X-ray crystallographic data. The ^1H–^{15}N NOE data indicate that the scF_v backbone has a well-defined structure of limited conformational flexibility. However, the linker of the scF_v fragment exhibits substantial fast internal motion (on the picosecond to nanosecond time scale) compared with the overall rotational correlation time of the whole molecule. Several residues in the CDRs, in turns, or at the C-terminal end of the protein have smaller NOEs, reflecting some degree of rapid motion in the protein backbone.

Although the three-dimensional structures of a number of F_{ab}[1] and F_v fragments of antibodies have been determined by X-ray crystallography (Davies et al., 1990; Alzari et al., 1988), other techniques are required to gain information about the structural and dynamic properties of the molecule (Wüthrich, 1986). NMR is particularly informative, as it not only allows the determination of the structure in solution but also allows the study of dynamic processes in proteins (Kay et al., 1989; Takahashi et al., 1992; Constantine et al., 1993). Such dynamic processes are important in studies of antibodies for understanding adaptive changes upon antigen binding and "thermal breathing" of the molecule and the investigation of folding reactions. We now report the assignment and secondary structure in solution of the antigen-binding fragment of an antibody. Previous NMR studies have been carried out on various aspects of antibody–antigen interactions (Anglister, 1990; Odaka et al., 1992; Tsang et al., 1991; Wright et al., 1990). Assignments of residues in the binding site (Anglister et al., 1989; McManus et al., 1991; Takahashi et al., 1991) or of one chain (Constantine et al., 1992; Goldfarb et al., 1993) have recently been obtained. However, no extensive assignments of backbone ^1H and ^{15}N resonances for a whole F_v fragment have been reported so far.

The F_v fragment (consisting of a heterodimer of V_L (115 amino acids) and V_H (122 amino acids)) of the phosphorylcholine-binding antibody McPC603 (Perlmutter et al., 1984), the smallest part of the antibody still containing the complete binding site, was used in this study. Additionally, both domains were linked to give the single-chain F_v fragment (V_H–$(Gly_4$-$Ser)_3$–V_L, 252 amino acids) (Bird et al., 1988; Huston et al., 1988; Glockshuber et al., 1990). For a detailed NMR study of a protein of this size, extensive isotope labeling must be performed to obtain ^{15}N- and ^{13}C-edited NMR spectra (Bax & Grzesiek, 1993; Fesik & Zuiderweg, 1990). The F_v fragment was secreted in functional form into the periplasm of *Escherichia coli* (Skerra & Plückthun, 1988; Plückthun, 1992), while the corresponding scF_v fragment was prepared from inclusion bodies in the cytoplasm of *E. coli* and refolded *in vitro* (Freund et al., 1993). Uniformly ^{15}N-labeled F_v fragment for the 3D double-resonance experiments was produced using the secretion process. The second method, which makes more efficient use of the label, was chosen for preparing selectively ^{15}N-labeled samples, as well as for the uniformly ^{15}N- and ^{13}C-labeled samples. The ^1H, ^{15}N, and ^{13}C spectra of the scF_v fragment exhibited broader line widths than those of the F_v fragment. Typical line widths were 30 Hz for a single-quantum magnetization of ^1H amide protons and 18 Hz for the heteronuclear multiple-quantum magnetization of ^{15}N backbone nitrogens in the ^{15}N-labeled scF_v samples. In the TOCSY-HMQC (Marion et al., 1989) spectrum about 50 $^1H^{\alpha}$ protons were identified. The HNCA

† This work was supported by research grants from the Bundesministerium für Forschung und Technologie and Grant PL 107/2-2.

‡ Max Planck Institute for Biochemistry.

§ University of Zürich.

® Abstract published in *Advance ACS Abstracts,* March 1, 1994.

[1] Abbreviations: F_{ab}, antigen-binding antibody fragment; F_v, antibody fragment composed of the variable heavy (V_H) and variable light (V_L) chain domains; scF_v, single-chain F_v fragment (a continuous protein of the structure V_H–linker–V_L); CDR, complementarity-determining region; HMQC, heteronuclear multiple-quantum coherence; HNCA, amide proton to nitrogen to α-carbon correlation; HN(CA)H, amide proton to nitrogen (via α-carbon) to α-proton and back to amide proton correlation; NMR, nuclear magnetic resonance; NOE, nuclear Overhauser effect; NOESY, two-dimensional NOE spectroscopy; TOCSY (HOHAHA), total correlation spectroscopy (homonuclear Hartmann–Hahn spectroscopy); TPPI, time- proportional phase incrementation; τ_m, rotational correlation time; T_2, transverse relaxation time.

0006-2960/94/0433-3296$04.50/0

(Kay et al., 1990) and HN(CA)H (Seip et al., 1992; Clubb et al., 1992) triple-resonance experiments yielded even fewer correlations due to the inherent short T_2 relaxation times of the ^{15}N and $^{13}C^{\alpha}$ in larger molecules (Ikura et al., 1990; Kay et al., 1992; Montelione & Wagner, 1990; Clubb et al., 1992; Boucher & Laue, 1992; Bax & Grzesiek, 1993), which limits the technique to proteins with molecular masses below 20 kDa (Kay et al., 1992). We show in this paper that it is still possible to obtain a high degree of assignment of the ^1H and ^{15}N resonances using a combination of residue-type-specific as well as domain-specific labeling and information obtained from the HMQC and NOESY-HMQC spectra (Muchmore et al., 1989; McIntosh & Dahlquist, 1990). Sequence-specific assignments were made and secondary structure elements defined from the 3D NOESY-HMQC spectrum. Dynamic information about most of the backbone NH groups of the F_v fragment was obtained using a modified method to measure the heteronuclear NOE between ^{15}N and ^1H.

MATERIALS AND METHODS

Protein Labeling and Sample Preparation. The expression and purification of the protein from *E. coli* was carried out as described previously (Freund et al., 1993; Figure 1S showing the different antibody fragments used in this study displayed on a polyacrylamide gel is available from the authors). F_v fragments were obtained by periplasmic secretion; scF_v fragments, from inclusion bodies refolded in vitro. scF_v fragments were used for obtaining uniformly ^{15}N–^{13}C-labeled protein as well as for ^{15}N-labeling with specific amino acids. F_v fragments were used for domain-specific and uniformly ^{15}N-labeled samples. The ^{15}N-amino acid specific labeling of scF_v was individually performed for ^{15}N-Ala, -Cys, -Gly, -Leu, -Lys, -Phe, -Ser, -Thr, -Tyr, and -Val. To prevent cross-labeling, all other amino acids were added in unlabeled form to the minimal medium (Senn et al., 1987). The ^{15}N-labeled amino acid was separately dissolved and passed through a sterile filter. One-half of the sample was added to the growth medium at the beginning of the fermentation; the rest was added at the time of induction (OD_{550} = 0.5). A certain extent of cross-labeling was however observed for some amino acids (C. Freund et al., in preparation). For the preparation of the ^{15}N-V_L-labeled F_v fragment and the ^{15}N-labeled V_L domain, the two chains of the uniformly ^{15}N- labeled F_v fragment as well as an unlabeled F_v fragment were separated under denaturing conditions on a CM–Sepharose column in 8 M urea and 5 mM MOPS, pH 7.0. A 0.1 mM solution of the ^{15}N-labeled, denatured V_L domain was either diluted 1:10 into refolding buffer (0.5 M arginine, 0.2 M Tris, and 5 mM EDTA, pH 9.5) to yield the isolated folded V_L domain dimer or mixed with a stoichiometric amount of the denatured, unlabeled V_H domain and then diluted 1:20 into the refolding buffer, yielding the ^{15}N-V_L–labeled F_v fragment.

Protein solutions were concentrated by centrifugation in Centricon-10 tubes at 2200*g*. NMR samples contained 1 mM protein, 1 mM phosphorylcholine, 1 mM EDTA, and 30 mM potassium phosphate, pH 6.0, in 90% H_2O/10% D_2O.

NMR Spectroscopy. All spectra were recorded at 27 °C on a Bruker AMX 600 spectrometer equipped with a multichannel interface and a BGU 10A gradient unit. All 3D NMR spectra were processed with our own software, CC-NMR (Cieslar et al., 1993). For recording the heteronuclear spectra, the ^1H carrier frequency was placed at the water resonance in dimensions for which the whole proton sweep width of 11.5 ppm was acquired. In the ^{15}N-edited proton dimension, where only the amide region was recorded, the carrier frequency was 7.57 ppm. The sweep width for covering the amide region of the proton spectrum was set to 5.75 ppm. The nitrogen carrier frequency was placed in the center of the backbone amides at 120 ppm (with respect to liquid ammonia); the sweep width in this dimension was 35.2 ppm. For the triple-resonance experiments, the carrier frequency was at the center of the α-carbon region at 55 ppm with respect to TMS. To encompass the whole chemical shift range of α-carbons in HNCA, the sweep width was set to 37 ppm. For the HN(CA)H correlation (Seip et al., 1992), the proton carrier was placed in the center of this region at 4.19 ppm during the evolution period of the α-proton. The sweep width was set to 4.00 ppm. For all experiments that involved coupling constants to ^{15}N, the nitrogen was decoupled during the acquisition by the GARP sequence (Shaka et al., 1983) with a field strength of 1 kHz. If necessary, presaturation of water was achieved with a field strength of 70 Hz and a duration of 1.3 s. Phase sensitivity in the acquisition dimension was achieved with the Bruker qsim mode, thus recording complex data points. Along all other dimensions TPPI was used for obtaining phase-sensitive spectra (Marion & Wüthrich, 1983).

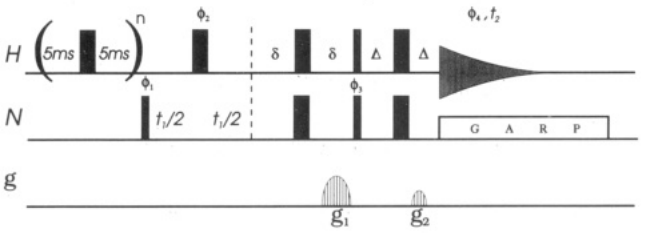

FIGURE 1: Pulse sequence for the measurement of the steady-state NOE between ^{15}N and ^1H. Details about pulses and gradient pulses (g) are given in the text. The phase cycling is as follows: $\Phi_1 = 8(x,-x)$; $\Phi_2 = (4(x),4(y),4(-x),4(-y))$; $\Phi_3 = 4(x,x,-x,-x)$; $\Phi_4 = 4(x,-x,-x,x)$. The delay δ was set to 2.75 ms; Δ = 2.4 ms.

Two-dimensional heteronuclear multiple-quantum coherence (HMQC) ^1H–^{15}N correlation spectra were acquired with standard methods (Summers et al., 1986). Three-dimensional ^{15}N-separated NOESY-HMQC spectra with a mixing time of 110 ms including a homospoil pulse of 8 ms (Zuiderweg & Fesik, 1990; Messerle, et al. 1989) and TOCSY-HMQC (Marion, et al., 1989) spectra with mixing times of 30 and 70 ms and 16 scans per t_1–t_2 pair were recorded. The size of the matrices was 160 × 52 × 2K data points. The MLEV-17 sequence (Bax & Davis, 1985; Davis & Bax, 1985), embraced by two hard spin lock pulses of 1.5 ms, was used in the TOCSY-HMQC experiment; the clean-TOCSY was utilized to avoid ROESY peaks (Griesinger et al., 1988). The 17th pulse of the MLEV sequence had a flip angle of 60°. The proton carrier frequency for isotropic mixing was placed between the amide and α-proton resonances at 6.43 ppm. To prevent sample heating, the power of the MLEV pulses was reduced by 6 dB. For the HNCA triple-resonance experiment (Ikura et al., 1990; Kay et al., 1990), the size of the data matrix was 64 × 64 × 2K data points and 48 scans were applied. In the case of the HN(CA)H experiment, the size of the matrix was 52 × 17 × 2K data points and 128 scans were accumulated. Presaturation was used for water suppression in all three-dimensional experiments.

The pulse sequence for measuring the heteronuclear NOE is a modification of a scheme proposed by Ross et al. (1993b) and is shown in Figure 1. Because of the broad line width of ^{15}N signals of F_v (16 Hz), the constant time delay in the original pulse sequence was replaced by an evolution time t_1 incremented in a standard manner and followed by a refocused

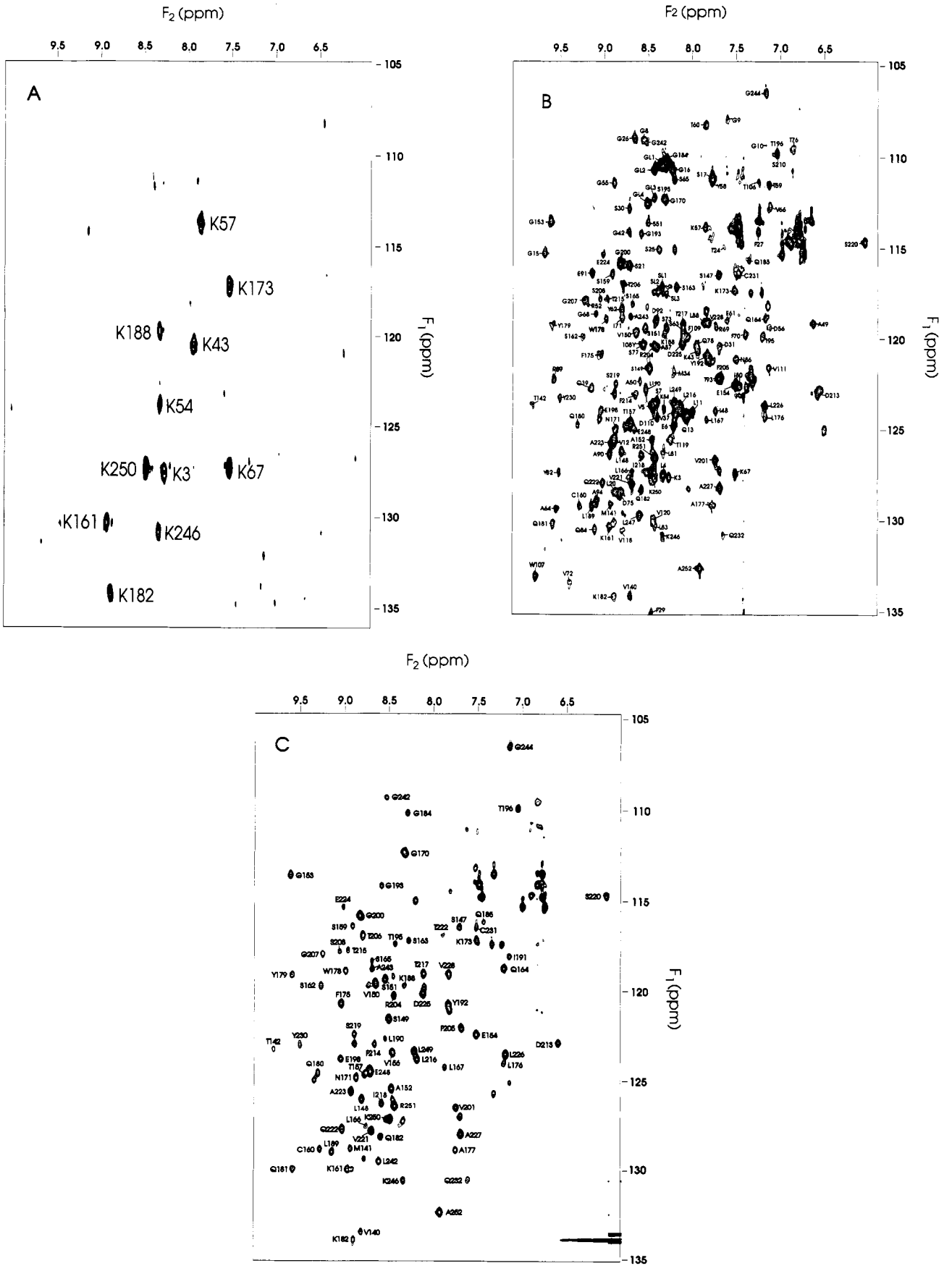

FIGURE 2: (A) ^{15}N–^{1}H HMQC spectrum of a selectively ^{15}N-lysine-labeled scF_v sample. The number of peaks in the spectrum corresponds to the number of lysines within the protein (11). (B) ^{15}N–^{1}H HMQC spectrum of the uniformly labeled scF_v. Assigned residues are marked within the spectrum. Linker residues which were sufficiently resolved (7 out of 15) are numbered arbitrarily (GL1–GL4 and SL1–SL3), since no sequence-specific assignment was possible. (C) ^{15}N–^{1}H HMQC spectrum of the ^{15}N-V_L-labeled F_v. Residue numbers are given in correspondence to the scF_v, where the V_L domain starts at position 138.

INEPT block. Gradient pulses were used for both coherence selection and water suppression. Positions of the gradients are shown in Figure 1. Each gradient had the shape of a sine function 1 ms in length. No further delays had to be included in the sequence, thus avoiding large phase errors in the final spectra. To achieve phase sensitivity along F_1, two data sets were recorded with alternation of the sign of the first (defocusing) gradient for each increment. Processing of such data to one States-like data set is described by Ross et al. (1993a). To extract heteronuclear NOEs, two measurements were recorded: the first spectrum was acquired with a broad-band presaturation of protons, thus achieving the NOE enhancement, and the second spectrum was taken without the presaturation (the reference spectrum). For the broad-band presaturation of the amides, a sequence of 120° pulses spaced by 10 ms was applied for a duration of 3 s. To ensure the same equilibrium state for the reference experiment, the relaxation delay between the scans had the same length as the total presaturation sequence. The size of the acquired data matrix was 188 × 2K data points, which were transformed to spectra with 256 × 2K points, using qsine and Gaussian windows along t_1 and t_2, respectively.

An amide-exchange experiment, consisting of a series of HMQC experiments, was carried out with the scF_v fragment lyophilized from aqueous buffer and then freshly dissolved in D_2O. Within 24 h, 20 2D data sets were recorded, each consisting of 128 t_1 increments with eight scans each. The whole data set was processed as a pseudo-3D experiment.

RESULTS AND DISCUSSION

NMR spectra have been recorded from the F_v and the scF_v fragment of the antibody McPC603. As we have shown previously, the linker does not perturb the folding of the domains (Freund et al., 1993). A comparison of a 2D ^1H–^{15}N HMQC spectrum of the ^{15}N-labeled single-chain F_v with a HMQC spectrum of the ^{15}N-labeled F_v sample revealed that all ^1H–^{15}N correlations align precisely in both spectra, with the exception of the additional correlations from the linker residues. It was therefore possible to make use of both structures in the assignment.

Strategy of the Assignment. The following considerations were taken into account in designing our approach for the assignment of the F_v spectra. Assignment techniques using the ^{15}N–^{13}C-edited spectra were not possible because of broad lines in the spectra of the ^{15}N-^{13}C doubly labeled sample. In the HNCA experiment, the line width of $^{13}C^{\alpha}$ peaks was 40–50 Hz and the J_{CC} coupling with $^{13}C^{\beta}$ was not resolved. In the initial stages of our work, we tried an approach similar to that of Constantine et al. (1992) of first assigning the isolated V_L (or V_H) domain alone. While this paper was in preparation, a communication appeared that described assignments of NMR resonances of the V_L domain of the F_v fragment of the anti-digoxin antibody 26-10 (Goldfarb et al., 1993) using a reconstituted F_v ^{15}N-labeled exclusively in the V_L domain, together with the already available assignments of the isolated V_L domain (Constantine et al., 1992). However, in the case of V_L of the McPC603 antibody, the line widths in the NMR spectra indicated that the isolated V_L is dimeric in solution at a concentration of 1 mM, with some extra line broadening presumably due to aggregation. This was expected since V_L of McPC603 is dimeric in the crystal state (Steipe et al., 1992). The V_H domain by itself showed low solubility, and ^1H line widths of the V_H domain were very broad due to aggregation. We have therefore chosen the more laborious, but promising, method of selective labeling in order to gain

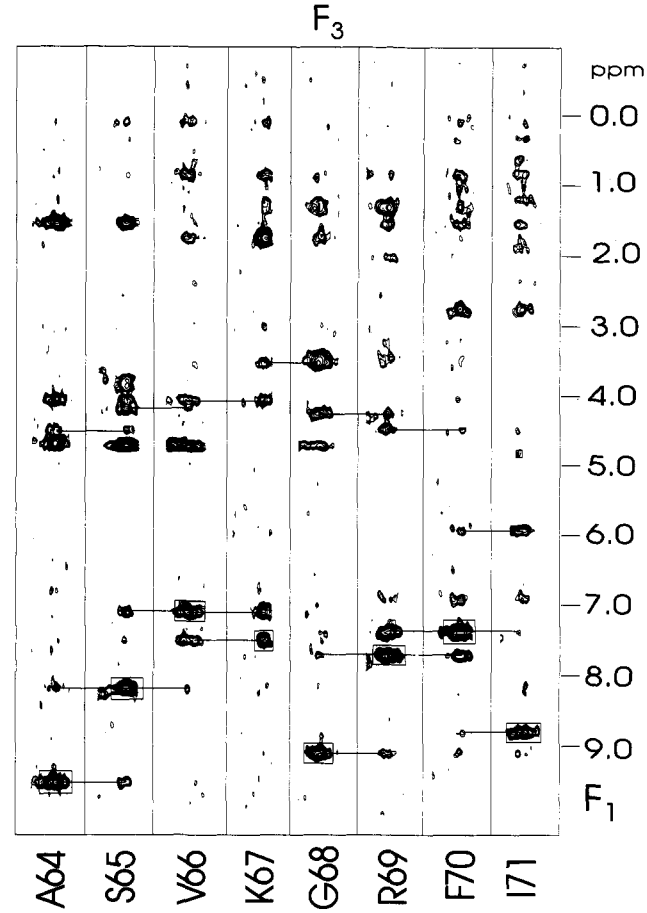

FIGURE 3: Strips from the 3D NOESY-HMQC spectrum of the F_v fragment, showing resonances of residues A64–I71, belonging to CDR2 and the beginning of β-strand 6 of the V_H domain. The strips, 65–70 Hz wide, are taken at the ^{15}N and ^{15}NH chemical shifts of interest. Rectangles mark the NH diagonal peaks, and solid lines indicate sequential NH(*i*)–NH(*i* – 1) and NH(*i*)–C$^{\alpha}$H(*i* – 1) connectivities.

the necessary residue- and domain-specific information. Sequence-specific assignments using sequential NOEs in the 3D NOESY-HMQC spectrum sometimes turned out to be ambiguous, but the high degree of regular secondary structure (β-sheets) allowed us to overcome these difficulties in most cases due to the observation of medium- and long-range NOEs that could confirm tentative assignments obtained from the sequential NOEs.

Residue- and Domain-Specific Assignments. Two 3D TOCSY-HMQC spectra were recorded. One spectrum with a short mixing time of 30 ms was used for most assignments in order to minimize relaxation effects and to obtain as many NH to C$^{\alpha}$H correlations as possible. The longer mixing time of 70 ms resulted in fewer NH to C$^{\alpha}$H transfers, but some additional NH to C$^{\beta}$H proton transfers became visible. Nevertheless, the identification of the spin systems could not be achieved using the 3D TOCSY-HMQC spectrum, except for a few glycine and alanine residues. Spin systems were therefore identified mostly by residue-specific labeling. In each experiment, one or two residue types were ^{15}N-labeled in the amide position (an example is given in Figure 2A for the ^{15}N labeling of lysines). A comparison of the HMQC spectra of these scF_v samples with the HMQC spectrum of the uniformly labeled F_v (or scF_v) (Figure 2B) allowed identification of the respective peaks from the ^{15}N-labeled amino acid in the HMQC and 3D NOESY-HMQC spectra of the uniformly labeled F_v (or scF_v). Alignment of the HMQC spectrum of the ^{15}N-V_L domain labeled F_v (Figure 2c) with

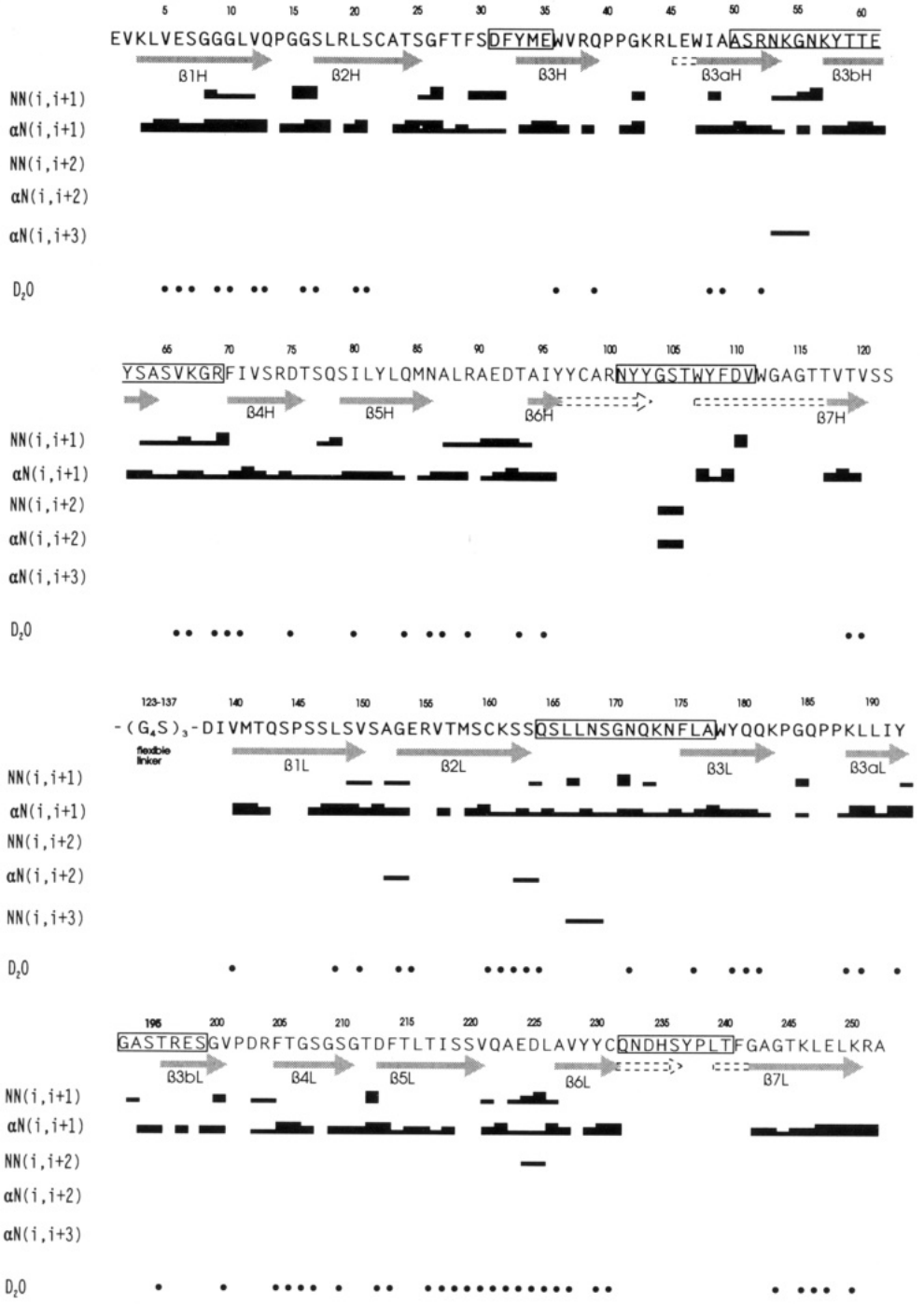

FIGURE 4: Summary of the short-range NOEs. The height of the bar used to denote an NOE is an indication of its intensity. Circles indicate slowly exchanging NH protons that persist for at least 24 h in D_2O solutions. Possible extensions of β-strands are indicated by dashed lines. CDR residues are boxed within the sequence. The β-strands are denoted according to the convention used by Branden and Tooze (1991).

the HMQC spectrum of the uniformly labeled F_v resulted in domain-specific assignment. Amino acid specific assignment was thus achieved for 140 residues, and the domain-specific differentiation could be obtained for almost all well-resolved ^{15}N–^1H peaks ($\sim$180).

Sequential Assignment of the ^1H and ^{15}N Resonances. Figure 3 shows an example of the sequential assignment in the 3D NOESY-HMQC spectrum for residues Ala 64 to Ile 71. The sequential assignment was started with the NH–$C^\alpha H$ connectivities. Most of the residues showed a strong NH(i)–$C^\alpha H(i-1)$ and a weak NH(i)–$C^\alpha H(i)$ cross peak. Additional $C^\beta H(i-1)$– or $C^\gamma H(i-1)$– NH(i) cross peaks could often be identified and served as further proof for the sequential assignment. Segments comprising turns or the CDRs also displayed sequential NH–NH peaks (Figure 3). By this procedure, sequence fragments varying in length from three to nine residues were found. Sequence-specific assignment was then often straightforward, because part of these segments contained several residues identified by residue- and domain-specific labeling.

Secondary Structure. Figure 4 summarizes the sequential and short-range NOEs observed in the NOESY-HMQC spectrum of the F_v fragment. These NOEs are the basis for the determination of the secondary structure of the protein (Wüthrich et al., 1984; Wüthrich, 1986). The β-strands were identified by strong sequential $C^\alpha H(i)$–NH($i+1$) and weak intraresidue $C^\alpha H(i)$–NH(i) cross peaks. Additionally, these peaks often displayed low- field $C^\alpha H$ and NH chemical shifts

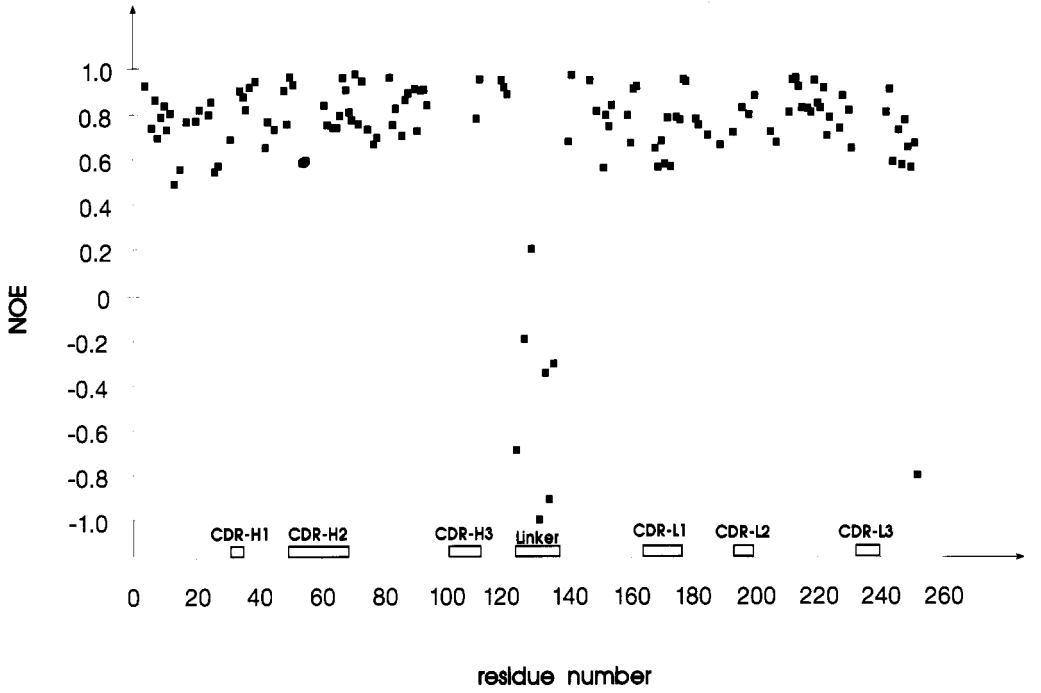

FIGURE 5: Plot of the observed ^{15}N NOE versus the amino acid sequence of the scF_v fragment.

and reduced NH exchange rates. The β-sheet structure was indicated by cross-strand NOEs between $C^{\alpha}H(i)$ and NH(j) or NH(i) and NH(j) (see the supplementary material). A large number of the NOEs in the NH–NH region of the NOESY-HMQC spectrum were due to cross-strand NOEs between residues involved in β-sheet structure. This phenomenon has been observed for other β-sheet proteins (Stockman et al., 1992). Eighteen β-strands could be identified comprising residues 3–13, (16)18–25, 34–39, (45)48–53, 57–64, 70–76, 79–86, 94–96(103), (107)117–120, 140–150, 153–163, 175–182, 187–192, 196–201, 205–211, 213–221, 227–232(236), and (239)242–250, respectively (Figure 4). For β-strands β3aH, β6H, β7H, β6L, and β7L (Figure 4) the most probable delineation of the beginning and/or the end of the β-strand is given. The residue numbers in parentheses indicate the largest possible length of the strand that could still be obtained from the present NMR data. The determination of the ends of these strands is not precise because of the incompleteness of the assignment, the spectral overlap, and/or the lack of diagnostic NOEs. The pattern of long-range NOEs indicated that most β-strands form antiparallel β-sheet structure, with the exception of residues G10–V12 and V118–V120 as well as S147–S151 and K246–K250, which form short parallel β-sheets.

CDRs and turns were characterized by sequential NH to NH, i to $i + 2$ or i to $i + 3$ contacts (Figures 3 and 4). Most of the turns were short, and the chemical shift values often lie between the average values for β-strand and coil structures (Wishart et al., 1991). An exception were the turns L88–T93 (V_H) and S220–L226 (V_L), which connect the β-strands β5H–β6H and β5L–β6L, respectively (Figure 4). Residues within these two turns were well defined, showed strong connectivities with each other, and had slowly exchanging amide protons. Similar observations were made for residues A64–F70, which connect the β-strands β3bH and β4H and are part of the CDR2 of the V_H domain (Figure 4). Despite the lack of an assignment of some resonances (due to overlap problems), CDR1 of V_H (D31–E35) and CDRs 1 and 2 of V_L (Q164–A177 and G193–S199) could also be reasonably well defined. The CDR3s of both domains are only poorly defined, raising the question of whether this lack of information is due to an intrinsic dynamic property of these CDRs (for example, slow exchange of two or more conformations).

The secondary structure elements in solution show the same pattern as in the X-ray structure (Figure 5 in Satow et al. (1986)). According to the X-ray structure, the first β-strands of both domains display characteristic structural abnormalities since the first and second parts of these strands bind to two different faces of the β-barrel. This is also observed in solution. A kink at position G9 slightly disrupts the strand β1H and gives rise to unusual NH–NH connectivities between neighboring residues (Figure 4). A *cis*-proline at position 145 that separates strand β1L (Figure 4) into two parts could also be detected by NMR. For a few β-strands, especially those comprising parts of CDR3 of both domains (above), only β-segments shorter than the ones seen in the X-ray structure could be assigned by NMR. Interestingly, CDR1 of the V_L domain, which is poorly defined in the X-ray structure, could be completely assigned in the NOESY-HMQC spectrum and displays sequential as well as medium-range NOEs.

Domain–Domain Interaction in the F_v Fragment. The V_H–V_L interaction is expected to be a major factor of stabilization in the F_v fragment. In fact, upon heterodimerization (V_L–V_H), there were large changes in the chemical shift values for many residues as compared to those that occur upon homodimerization (V_L–V_L) (data not shown). As expected, most of the residues displaying these large chemical shift differences are at the V_L–V_H interface, in agreement with the data obtained for another F_v fragment (Goldfarb et al., 1993). However, only a few NOEs between the domains could be observed.

Dynamic Properties. The experimental ^{15}N NOE values are plotted against the amino acid sequence in Figure 5. Accurate peak height measurements were possible for 133 resonances from the total of 180 resolved peaks. The average value of the NOEs was 0.80. There were 109 residues with NOEs within 20% of the average value (Figure 5). These values mean that most of the scF_v backbone exists in a well-defined structure of limited conformational flexibility (on the nano- to picosecond time scale), with any motions faster than τ_m being of small magnitude (Lipari & Szabo, 1982a,b; Kay

et al., 1989; Clore et al., 1990a,b; Palmer et al., 1991; Barbato et al., 1992; Berglund et al., 1992; Kördel et al., 1992; Redfield et al., 1992; Stone et al., 1992; Schneider et al., 1992; Cheng et al., 1993). The exception is the linker segment, which exhibits negative NOEs that reflect a significant degree of rapid motion in the protein backbone. These data, combined with the $^3J_{NH-H\alpha}$ coupling constants of 7 Hz (Wüthrich, 1986), indicate that the linker residues are random structures. The only other residue with a negative NOE is the C-terminal residue A252. Residues displaying NOE values more than 25% smaller than the average value were Q13, G15, S26, F27, K54, G55, S151, S169, N171, K173, G244, L247, and R250. These residues are within the CDRs, in turns, or at the C-terminal end of the protein. It has to be pointed out that other residues of the CDRs (e.g., M34, E61, A64, S65, V66, G70, Q172, and F175) have NOE values close to the average value of 0.8. Therefore, flexibility in the CDRs is not uniform but rather strictly localized to certain positions.

In conclusion, we have shown that it is possible to obtain assignment of about 80% of the ^{15}N and ^1H backbone and 60% of the ^1H side-chain resonances in an F_v fragment and a scF_v fragment of an antibody, a protein of 252 amino acids. It is also possible to identify the solution secondary structure elements in a β-sheet protein of this size as a large portion of the NOEs in the NH–NH region of the NOESY-HMQC spectrum are due to cross-strand NOEs between residues involved in β-sheet structure. The ^{15}N NOE data indicate that the F_v backbone has a well-defined structure of limited conformational flexibility. In contrast, the linker exhibits substantial fast internal motion compared with the overall rotational correlation time of the whole molecule. There are also several residues within the CDRs, in turns, or at the C-terminal end of the protein with clearly smaller NOEs reflecting some degree of rapid motion in the protein backbone.

SUPPLEMENTARY MATERIAL AVAILABLE

A table of the ^1H and ^{15}N assignments, a list of the long-range NOEs used to determine the interstrand structure of β-sheets, a table with values of the NOE for the scF_v fragment, and a table comparing the numbering scheme used in this study with those used in the X-ray structure and the nomenclature of Kabat et al. (1991) (11 pages). Ordering information is given on any current masthead page.

REFERENCES

Alzari, P. M., Lascombe, M. B., & Poljak, R. J. (1988) *Annu. Rev. Immunol. 6*, 555–580.

Anglister, J. (1990) *Q. Rev. Biophys. 23*, 175–203.

Anglister, J., Levy, R., & Scherf, T. (1989) *Biochemistry 28*, 3360–3365.

Barbato, G., Ikura, M., Kay, L. E., Pastor, R. W., & Bax, A. (1992) *Biochemistry 31*, 5269–5278.

Bax, A., & Davis, D. G. (1985) *J. Magn. Reson. 65*, 355–366.

Bax, A., & Grzesiek, S. (1993) *Acc. Chem. Res. 26*, 131–138.

Berglund, H., Kovacs, H., Dahlman-Wright, K., Gustaffson, J-Å., & Härd, T. (1992) *Biochemistry 31*, 12001–12011.

Bird, R. E., Hardman, K. D., Jacobson, J. W., Johnson, S., Kaufman, B. M., Lee, S., Lee, T., Pope, S. H., Riordan, G. S., & Whitlow, M. (1988) *Science 242*, 423–426.

Boucher, W., & Laue, E. D. (1992) *J. Am. Chem. Soc. 114*, 2262–2264.

Branden, C., & Tooze, J. (1991) *Introduction to Protein Structure*, Chapter 12; Garland Publishing, Inc., New York.

Cheng, J.-W., Lepre, C. A., Chambers, S. P., Fulghum, J. R., Thomson, J. A., & Moore, J. M. (1993) *Biochemistry 32*, 9000–9010.

Cieslar, C., Ross, A., Zink, T., & Holak, T. A. (1993) *J. Magn. Reson. B101*, 97–101.

Clore, G. M., Driscoll, P. C., Wingfield, P. T., & Gronenborn, A. M. (1990a) *Biochemistry 29*, 7387–7401.

Clore, G. M., Szabo, A., Bax, A., Kay, L., Driscoll, P. C., & Gronenborn, A. M. (1990b) *J. Am. Chem. Soc. 112*, 4989–4991.

Clubb, R. T., Thanabal, V., & Wagner, G. (1992) *J. Biomol. NMR 2*, 203–210.

Constantine, K. L., Goldfarb, V., Jeffrey, P. D., Sheriff, S., & Mueller, L. (1992) *Biochemistry 31*, 5033–5043.

Constantine, K. L., Friedrichs, M. S., Goldfarb, V., Jeffrey, P. D., Sheriff, S., & Mueller, L. (1993) *Proteins 15*, 290–311.

Davies, D., Padlan, E. A., & Sheriff, S. (1990) *Annu. Rev. Biochem. 59*, 439–473.

Davis, D. G., & Bax, A. (1985) *J. Am. Chem. Soc. 107*, 2821–2822.

Fesik, S. W., & Zuiderweg, E. R. P. (1990) *Q. Rev. Biophys. 23*, 97–131.

Freund, C., Ross, A., Guth, B., Plückthun, A., & Holak, T. A. (1993) *FEBS Lett. 320*, 97–100.

Glockshuber, R., Malia, M., Pfitzinger, I., & Plückthun, A. (1990) *Biochemistry 29*, 1362–1367.

Goldfarb, V., Wittekind, M., Jeffrey, P. D., Mueller, L., & Constantine, K. L. (1993) *J. Mol. Biol. 232*, 15–22.

Griesinger, C., Otting, G., Wüthrich, K., & Ernst, R. R. (1988) J. Am. Chem. Soc. 110, 7870–7872.

Huston, S. J., Mudgett-Hunter, M., Tai, M. S., Novotny, J., Margolies, M. N., Ridge, R. J. Bruccoleri, R. E., Haber, E., Crea, R., & Oppermann, H. (1988) *Proc. Natl. Acad. Sci. U.S.A. 85*, 5879–5883.

Ikura, M., Kay, L. E., & Bax, A. (1990) *Biochemistry 29*, 4659–4667.

Kabat, E. A., Wu, T. T., Perry, H. M., Gottesman, K. S., & Foeller, C. (1991) *Sequences of Proteins of Immunological Intrest*, 5th ed., National Institutes of Health, Bethesda, MD.

Kay, L. E., Torchia, D. A, & Bax, A. (1989) *Biochemistry 28*, 8972–8979.

Kay, L. E., Ikura, M., Tschudin, R., & Bax, A. (1990) *J. Magn. Reson. 89*, 496–514.

Kay, L. E., Wittekind, M., McCoy, M. A., Friedrichs, M. S., & Mueller, L. (1992) *J. Magn. Reson. 98*, 443–450.

Kördel, J., Skelton, N. J., Akke, M., Palmer, A. G., III, & Chazin, W. J. (1992) *Biochemistry 31*, 4856–4866.

Lipari, G., & Szabo, A. (1982a) *J. Am. Chem. Soc. 104*, 4546–4559.

Lipari, G., & Szabo, A. (1982b) *J. Am. Chem. Soc. 104*, 4559–4570.

Marion, D., & Wüthrich, K. (1983) *Biochem. Biophys. Res. Commun. 113*, 967–974.

Marion, D., Driscoll, P. C., Kay, L. E., Wingfield, P. T., Bax, A., Gronenborn, A. M., & Clore, G. M. (1989) *Biochemistry 28*, 6150–6153.

McIntosh, L. P., & Dahlquist, F. W. (1990) *Q. Rev. Biophys. 23*, 1–38.

McManus, S., & Riechmann, L. (1991) *Biochemistry 30*, 5851–5857.

Messerle, B. A., Wider, G., Otting, G., Weber, C., &. Wüthrich, K. (1989) *J. Magn. Reson. 85*, 608–613.

Montelione, G., & Wagner, G. (1990) *J. Magn. Reson. 87*, 183–188.

Muchmore, D. C., McIntosh, L. P., Russell, C. B., Anderson, D. E., & Dahlquist, F. W. (1989) *Methods Enzymol. 177*, 44–73.

Odaka, A., Kim, J. I., Takahashi, H., Shimada, I., & Arata, Y. (1992) *Biochemistry 31*, 10686–10691.

Palmer, A. G., III, Rance, M., & Wright, P. E. (1991) *J. Am. Chem. Soc. 113*, 4371–4380.

Perlmutter, R. M., Crews, S. T., Douglas, R., Sorensen, G., Johnson, N., Nivera, N., Gearhart, P. J., & Hood, L. (1984) *Adv. Immunol. 35*, 1–37.

Plückthun, A. (1992) *Immunol. Rev. 130*, 151–188.

Redfield, C., Boyd, J., Smith, L. J., Smith, R. A. G., & Dobson, C. M. (1992) *Biochemistry 31*, 10431–10437.
Ross, A., Czisch, M., Cieslar, C., & Holak, T. A. (1993a) *J. Biomol. NMR 3*, 215–224.
Ross, A., Czisch, M., Zink, T., & Holak, T. A. (1993b) *J. Magn. Reson. B* (in press).
Satow, Y., Cohen, G. H., Padlan, E. A., & Davies, D. R. (1986) *J. Mol. Biol. 190*, 593–604.
Schneider, D. M., Dellwo, M. J., & Wand, J. A. (1992) *Biochemistry 31*, 3645–3652.
Seip, S., Balbach, J., & Kessler, H. (1992) *J. Magn. Reson. 100*, 406–410.
Senn, H., Eugster, A., Otting, G., Suter, F., & Wüthrich, K. (1987) *Eur. Biophys. J. 14*, 301–306.
Shaka, A. J., Barker, P. B., & Freeman, R. (1983) *J. Magn. Reson. 64*, 547–552.
Skerra, A., & Plückthun, A. (1988) *Science 240*, 1038–1041.
Steipe, B., Plückthun, A., & Huber, R. (1992) *J. Mol. Biol. 225*, 739–753.
Stockmann, B. J., Scahill, T. A., Roy, M., Ulrich, E. L., Strakalaitis, N. A., Brunner, D. P., Yem, A. W., & Deibel, M. R., Jr. (1992) *Biochemistry 31*, 5237–5245.
Stone, M. J., Fairbrother, W. J., Palmer, A. G., III, Reizer, J., Saier, M. H., Jr., & Wright, P. E. (1992) *Biochemistry 31*, 4394–4406.
Summers, M. F., Marzilli, L. G., & Bax, A. (1986) *J. Am. Chem. Soc. 108*, 4285–4294.
Takahashi, H., Odaka, A., Kawaminami, S., Matsunaga, C., Kato, K., Shimada, I., & Arata, Y. (1991) *Biochemistry 30*, 6611–6619.
Takahashi, H., Suzuki, E., Shimada, I., & Arata, Y. (1992) *Biochemistry 31*, 2464–2468.
Tsang, P., Rance, M., & Wright, P. E. (1991) *Methods Enzymol. 203*, 241–261.
Wishart, D. S., Sykes, B. D., & Richards, F. M. (1991) *J. Mol. Biol. 222*, 311–333.
Wright, P. E., Dyson, H. J., Lerner, R. A., Riechmann, L., & Tsang, P. (1990) *Biochem. Pharmacol. 40*, 83–88.
Wüthrich, K. (1986) *NMR of Proteins and Nucleic Acids*, J. Wiley, New York.
Wüthrich, K., Billeter, M., & Braun, W. (1984) *J. Mol. Biol. 180*, 715–740.
Zuiderweg, E. R. P., & Fesik, S. W. (1990) *Biochemistry 28*, 2387–2391.